HYDROMECHANICALLY COUPLED ANALYSIS OF TRANSIENT PHENOMENA IN A RAINFALL-INDUCED LANDSLIDE

J. Eichenberger[1]

M. Nuth[1]

L. Laloui[1]

Laboratory of Soil Mechanics, Ecole Polytechnique Fédérale de Lausanne, EPFL, Lausanne, Switzerland

ABSTRACT: *Heavy rainfall can lead to shallow slips in slopes that are initially in a state of partial water saturation. Multiphysics numerical modelling approaches taking into account the involved physical key processes in variably saturated soils during rainfall events could help in understanding the main slip mechanisms. The concerned processes are related to water flow through the solid matrix, soil water retention behaviour and the effects of matric suction on the mechanical behaviour. In this paper, the elasto-plastic constitutive model ACMEG-s that captures some key features of the behaviour of variably saturated soils is used in a fully coupled hydromechanical finite element analysis for the assessment of destabilizing, transient processes in a steep slope during rain infiltration. It is shown that at the onset of failure, wetting pore collapse and plastic shear strains occur in the lower part of the slope and develop upwards towards the slope surface to delimit a probable failure mechanism.*

1 INTRODUCTION

Rainfall-induced landslides are mostly superficial and are triggered in soil slopes where a permanent groundwater table is often absent due to slope steepness and generally dry environmental conditions. Soils in such slopes are most of the time in a state of partial water saturation. The failure surface of shallow slips is commonly situated between 0.5 and 3 meters in soil depth and runs subparallel to the slope surface along an interface between soil cover and bedrock. The whole sliding mass is often several meters to tens of meters wide, several tens of meters long and sums up to a couple of hundred to thousand cubic meters in volume (Dai et al. 1999). Shallow slides in steep (30 to 40°), loose colluvial deposits are mostly translational and mobilize completely to form debris flows. Actually, flow-type failures such as debris flows and flowslides are reported to result most often from shallow slips (Iverson et al. 1997). Although landslides under the action of variations of positive (compressive) pore pressures are well documented and probably most recurrent, they may also happen in unsaturated conditions. Such is the case for slopes where the substratum is not in particular less permeable than the soil cover and the contribution of capillary forces to slope stability is substantial (Godt et al. 2009).

In order to perform a geomechanical analysis of shallow landslide phenomena, the numerical model has to be capable of reproducing the physical processes during rain infiltration and failure initiation in variably saturated soils. Within the framework of an elasto-plastic constitutive model for unsaturated soils, results from a time-dependent, hydromechanical finite element analysis of a rainfall-induced landslide are presented in this paper. The considered case study is inspired from a real test-site slope in partially saturated

conditions subjected to rain infiltration (Springman et al. 2009). The simulation results show the usefulness of considering partial saturation in hydraulic and mechanical terms for the modelling of the predominant transient processes and key physical mechanisms, such as soil hardening effect of matric suction, wetting pore collapse and plastic shearing.

2 PHYSICAL PROCESSES IN UNSATURATED SOIL SLOPES

Commonly, two flow regimes are encountered in natural slopes: a deep flow regime, most often parallel to the slope surface with possible complex bedrock interactions and a superficial flow regime with capillary pressures or positive, compressive pore water pressures controlled by rainfall. The slope response to a rainfall event depends mainly on rainfall intensity and duration, on soil hydraulic characteristics, on the thickness of the sliding mass and on antecedent weather conditions (Klubertanz et al. 2009). The occurrence and type of landslide triggering mechanism depends strongly on hydraulic predisposition factors, but also on slope angle and mechanical soil characteristics. Shallow slope failures are often reported to occur along an interface between soil deposits and underlying bedrock under fully saturated conditions due to a build-up of positive pore water pressures and subsequent loss in soil shear strength (Johnson and Sitar 1990). This is especially the case for slopes where the effective internal friction angle of the soil is close to the slope angle. Slopes with an angle much steeper than the soil's internal friction angle rely on suction stresses and/or root reinforcement in order to be stable. In the case presented in this paper, the average slope angle is noticeably higher (α=38°) than the effective internal friction angle (φ'=33°) determined in the laboratory. A real-scale slope failure has been triggered artificially by sprinkling the test-site with water (Springman et al. 2009).

During a rainfall event, water infiltrates predominantly vertically under the influence of gravity and capillary forces into the soil. Several hydromechanical processes act in a destabilizing sense on the slope during and after rain infiltration:

- The degree of saturation of the upper soil layer increases, thereby reducing the capillary tension between the soil particles, which weakens in most cases the slope.
- Deposited soils, as well as heavily weathered residual soils are susceptible to a collapse of the loose soil matrix upon wetting. The wetting pore collapse in parts of the slope can lead to differential settlements (Jia et al. 2009). At high degrees of saturation, the rapid volume reduction may be a cause for debris flow initiation.
- A slope-parallel flow regime installs itself after the rainfall event in the upper partially saturated soil layer when the volume of infiltrated water is large enough. Water is consequently carried to the toe region. Upon that, due to the mobilized fluid flow inside the soil matrix, the fluid exerts a destabilizing, downhill frictional drag.

Unsaturated zone physical processes govern the time-dependent response of soil slope to a rainfall event. Considering that they take place in a timescale relevant to a single rainfall event, their identification and integration in the modelling process is necessary in order to perform an analysis of the onset of failure. This can be achieved with a hydromechanically coupled approach and an adequate constitutive model for variably unsaturated-saturated soils.

3 THEORETICAL FRAMEWORK FOR UNSATURATED SOILS

In order to capture the main features of soil slope behaviour in unsaturated conditions for modelling purpose, an elasto-plastic constitutive model including the soil water retention behaviour is used in the framework of hydromechanically coupled porous media. The principal model concepts are reviewed in this section.

The Advanced Constitutive Model for Environmental Geomechanics (ACMEG-s) (Nuth & Laloui 2007; Nuth & Laloui 2008a) is a Cam-Clay-type elasto-plastic model (Schofield & Wroth 1968) and is based on the so-called initial Hujeux's model (Hujeux 1985). The increment of strain $d\varepsilon_{ij}$ is decomposed into:

$$d\varepsilon_{ij} = d\varepsilon_{ij}^{e} + d\varepsilon_{ij}^{p} \tag{1}$$

Where $d\varepsilon_{ij}^{e}$ is the elastic strain increment and $d\varepsilon_{ij}^{p}$ the plastic strain increment. The elastic deformation can be expressed as:

$$d\varepsilon_{ij}^{e} = C_{ijkl} d\sigma'_{kl} \tag{2}$$

The tensor C_{ijkl} is the mechanical elastic tensor and is composed of non-linear elastic moduli. The elastic strain increment $d\varepsilon_{ij}^{e}$ can be decomposed in volumetric and deviatoric increments which are related to mean effective, respectively deviatoric stress by means of spherical stress-dependent elastic moduli. σ'_{kl} in Eq. (2) is the effective stress for unsaturated soils (Laloui & Nuth, 2009):

$$\sigma'_{kl} = \left(\sigma_{kl} - u_a \delta_{kl}\right) + S_r \left(u_a - u_w\right) \delta_{kl} \tag{3}$$

Where σ_{kl} is the total stress, u_a is the air pressure, u_w is the water pressure, S_r is the degree of saturation and δ_{kl} is the Kronecker's delta. The difference between the total stress σ_{kl} and the air pressure u_a is called the net stress $\sigma_{kl\,net}$. The difference between u_a and u_w is defined as the matric suction s.

The critical state line is defined in the plane of deviatoric stress q versus mean effective stress p', with a slope M. The slope of the critical state line in the plane volumetric plastic strain vs. mean effective stress $\left(\varepsilon_v^p - \ln p'\right)$ is β, p'_{CR0} being the initial critical state pressure:

$$\ln \frac{p'_{CR}}{p'_{CR0}} = \beta \varepsilon_v^p \tag{4}$$

In the ACMEG-s model, the plastic irreversible strain increment $d\varepsilon_{ij}^{p}$ is induced by two coupled dissipative processes: an isotropic and a deviatoric plastic mechanism. The yield limits of each mechanism, bounding the elastic domain in the effective stress space, can be written as:

$$\tilde{f}_{iso}(p', \varepsilon_v^p, r_{iso}) = p' - r_{iso}.d.p'_{CR} \tag{5}$$

$$\tilde{f}_{dev}(p', q, r_{dev}, \varepsilon_v^p, \varepsilon_d^p) = q - Mp'\left(1 - b \ln \frac{p'}{p'_{CR}}\right) r_{dev} \tag{6}$$

Where p'_{CR} is the critical state pressure. d, b, r_{iso} and r_{dev} are material parameters. ε_v^p and ε_d^p are respectively the volumetric plastic strain and the deviatoric plastic strain. The critical

state pressure in Eq. (4) can be related to the preconsolidation pressure $p_c^{'}$ using the material parameter *d*, that represents the distance in the volumetric plane between the normally consolidated line and the critical state line:

$$p'_c = d.p'_{CR} \tag{7}$$

Using the space of triaxial stress variables *q* and *p'*, the elastic domain is enclosed by an ellipsoidal surface which is cut by the isotropic yield limit (see Figure 1). Adding the suction s as a third axis of the space, Figure 1 shows that the elastic domain gets larger with suction. This accounts for the fact that a dryer material will have higher strength and stiffness. Eq. (8) gives the mathematical formulation of the contribution of the capillary effects to the mechanical behaviour. The principle is to introduce a dependency of the preconsolidation pressure p'_c on the level of suction s and using a material parameter γ_s:

$$p'_c = \begin{cases} p'_{c0} & \text{if } s \le s_e \\ p'_{c0}\left[1+\gamma_s \log\left(s/s_e\right)\right] & \text{if } s \ge s_e \end{cases} \tag{8}$$

p'_{c0} is the initial preconsolidation pressure at zero suction and s_e is the suction air entry.

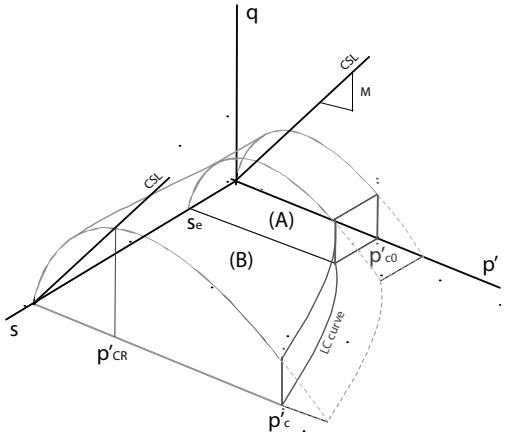

Figure 1. Yield surface shape and critical state line (CSL) in a $\left(p',q,s\right)$ space.

Modelling the evolution of the degree of saturation S_r with respect to suction s is also taken into account in the model (Nuth & Laloui 2008b). The increment of the degree of saturation dS_r is decomposed into an elastic part and a plastic part and is written:

$$dS_r = \frac{ds}{K_H \times \left(s/s_e\right)} + \frac{ds_D}{\beta_H \times \left(s_D/s_{D0}\right)} \tag{9}$$

K_H is the elastic slope and β_H is the plastic slope defined in Figure 2. s_e represents the limit below which the degree of saturation remains equal to one. s_e depends on the void ratio (i.e. the density of the material). If the suction remains lower than the air entry value, the degree of saturation equals one and there is no elastic increment. If the residual state is reached ($S_r = S_{res}$, where S_{res} is the residual degree of saturation), then the elastic increment becomes null too. s_D is the drying yield suction, which is the maximum suction ever

experienced by the material along a drying path. s_{D0} is the initial value of the drying yield suction.

The process of drying and wetting is not fully reversible and the $(S_r - s)$ data usually show the existence of a capillary hysteresis. A given level of suction can indeed correspond to different degrees of saturation. The way chosen to reproduce the retention hysteresis is to make the yield surface evolves by means of kinematic hardening. The elastic domain is delimited by the following yield limit:

$$f = \left\| \ln(s) - \ln(s_D) + \frac{1}{2}\left[\ln(s_{D0}) - \ln(s_e)\right] \right\| - \frac{1}{2}\left[\ln(s_{D0}) - \ln(s_e)\right] \tag{10}$$

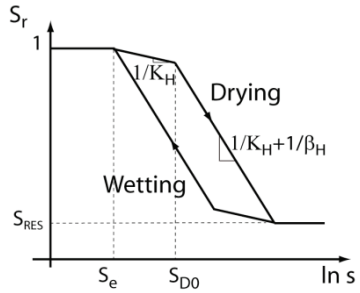

Figure 2. Modelling of the soil water retention curve.

For the flow problem, the generalized Darcy's law is used to describe the relative velocity of the fluid with respect to the solid skeleton. The permeability tensor $\mathbf{K}_w$ depends in general on the degree of saturation S_r. Assuming hydraulic isotropic conditions, the water relative permeability coefficient k_{rw} is defined according to the following relationship, CKW1 being a material parameter:

$$k_{rw} = \sqrt{S_r}\left[1 - \left(1 - S_r^{\frac{1}{CKW1}}\right)^{CKW1}\right]^2 \tag{11}$$

The constitutive model presented above is implemented into the finite element code called LAGAMINE (Charlier 1987; Collin 2003). The code features hydro-mechanically coupled finite elements.

4 NUMERICAL MODELLING OF AN UNSATURATED SOIL SLOPE SUBJECTED TO RAINFALL INFILTRATION

As a generic case study, the hydromechanically coupled analysis is inspired from realistic geometrical (Askarinejad 2009) and material parameters (Eichenberger et al., 2010) close to those of a real test-site case study in Rüdlingen, Switzerland (Swiss Competence Center Environment and Sustainability, project TRAMM). A detailed description of this landslide triggering experiment is presented by Springman et al. (2009). It is not intended here to reproduce the in-situ experiment neither to compare the performance of the model with the measured in-situ data. The material parameters for the ACMEG-s model were calibrated on the basis of triaxial, oedometer and retention tests carried out at the Laboratory of Soil Mechanics, EPFL (Table 1). The geometry of the slope is presented in Figure 3. The steep slope of 38° is composed of silty sand deposits (soil cover) of 2 to 5m thickness and a beneath laying, fractured bedrock. The principal objective of this study is to show the effect of rain infiltration on the stability of a partially saturated slope and its failure mechanisms.

4.1 Definition of the Geomechanical Model and the Calculation Procedure

The finite element mesh presented in Figure 3 is composed of 4672 six-noded quadratic triangles. The ACMEG-s constitutive model is applied to both, bedrock and soil cover, using the parameters of table 1. The behaviour of the bedrock is assumed elastic. Its saturated soil water permeability is set equal to that of the soil cover in order to focus the study solely on the effect of vertical rain infiltration and not on eventual hydraulic heterogeneities. The mesh is strongly refined in the upper soil layer in order to properly model the transient hydromechanical processes and the development of plastic zones during rain infiltration. Conventional kinematic boundary conditions are imposed to the box model.

Table 1. Parameters for the elasto-plastic ACMEG-s and water retention model.

		Symbol	Description	Value
Stress-strain model	Elastic parameters	K_{ref}	Bulk modulus	$1*10^9$ Pa
		G_{ref}	Shear modulus	$6*10^8$ Pa
		n^e	Elastic exponent	0.1
	Plastic parameters	φ'	Friction angle	33°
		β_0	Compressibility coefficient	30
		*α	Dilatancy coefficient	0.7
		*a		0.05
		b	see equation (5)	0.1
		*c		0.08
		d	see equation (4)	1.3
	Limits of elastic domain	r^e_{dev}	Initialisation of deviatoric mechanism	0.3
		r^e_{iso}	Initialisation of isotropic mechanism	0.3
Capillary effects		γ_s	Coefficient of LC curve	0.78173
		*Ω	Coef. var. compressibility	$2*10^{-5}$
		s_e	Air entry value	3000 Pa
Retention model		K_h	Elastic coefficient	8.8
		β_h	Plastic coefficient	10
		s_{D0}	Drying yield suction	6000 Pa
		S_{res}	Residual degree of saturation	0.3
Permeability		$k_{w,sat}$	Intr. water permeability	10^{-5} m/s
		CKW1	Parameter for the water rel. perm. function	0.55

*see Nuth & Laloui 2007 for explanation of parameters.

Initially, two calculations are run which consist of a gravity loading phase and a coupled flow and deformation analysis for the determination of the water table position and distribution of matric suction in the vadose zone. The resulting water table runs inclined from the top left to the bottom right model boundary. Matric suction is distributed hydrostatically in the partially saturated zone above the water table and the degree of saturation reaches its residual value of $S_r = 0.3$ along the slope surface, see Figure 3.

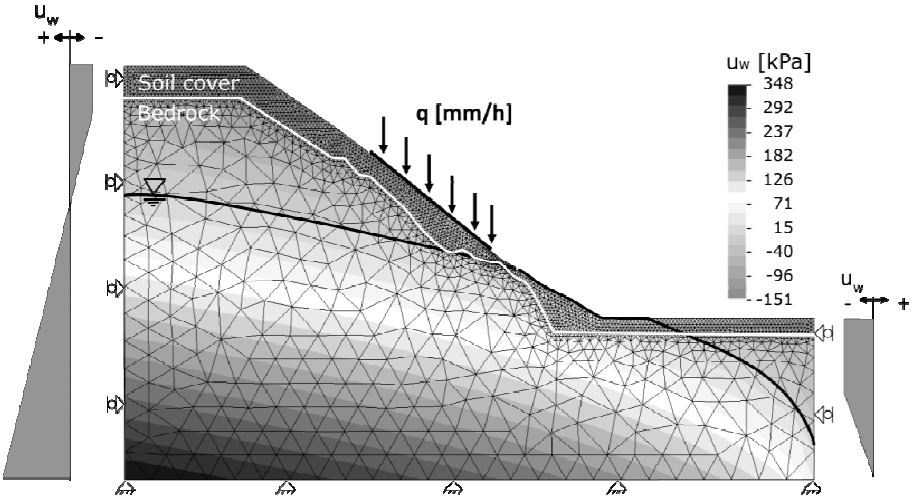

Figure 3. Finite element mesh, boundary and initial conditions.

In a final step, rain infiltration is simulated by means of an imposed boundary flux of 15mm/h for 3.5 days (the rain input is virtual and does not correspond to the real experiment). The water saturation contours in Figure 4a show clearly that the superficial soil layer has been quasi completely saturated. The soil water retention curve in Figure 4b indicates for 3 points at different depths that the matric suction has decreased to reach zero or close to zero values.

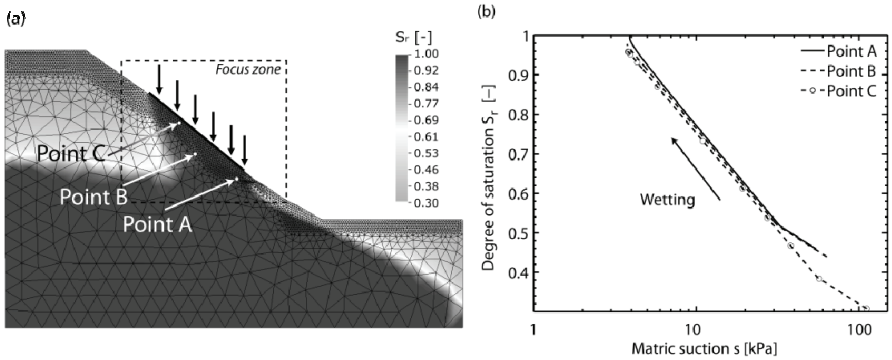

Figure 4. Rain infiltration in a partially saturated slope: spatial distribution of the degree of saturation (a); Soil water retention curve (b).

4.2 Plastic Mechanisms during Rain Infiltration

The supply of water in a partially saturated slope acts negatively on its stability. With increasing water content, the capillary forces reigning between the soil particles decrease. This de-bonding effect of wetting is taken into account in the model through the effective stress (Eq. (3)), which decreases during rain infiltration. The soil loses strength in classical soil mechanics terms.

In Figure 5, the contours of deviatoric strains are shown for the ”focus zone” indicated in Figure 4. Shear strains are localized along the interface between bedrock and soil layer for the lower and middle part of the slope and run up biased to the slope surface in the upper part. The extent of the shear zone coincides with the zone of increased degree of saturation (Figure 4a), showing clearly a localized effect of the infiltrated water.

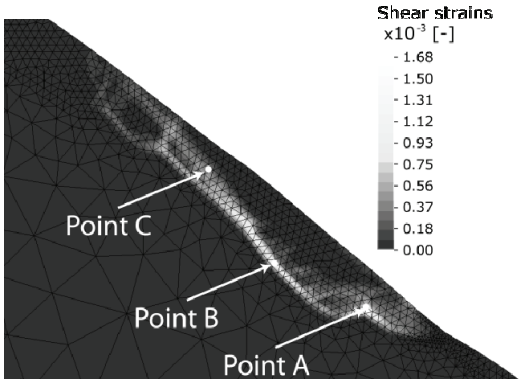

Figure 5. Contour of deviatoric strains after 3.5 days of rain infiltration. Light zones indicate a concentration of shear strains.

The deformation history of three selected points A, B and C defined in Figure 5 indicate which plastic mechanism, among the isotropic (Eq. (5)) and deviatoric (Eq. (6)), is predominant in different parts of the slope at different instants in time. The soil in the vicinity of point A above the bedrock abutment was almost normally consolidated prior to infiltration. In this zone, water infiltration is at the origin of strong shearing associated with noticeable positive (compressive) plastic volumetric deformations (Figure 6).

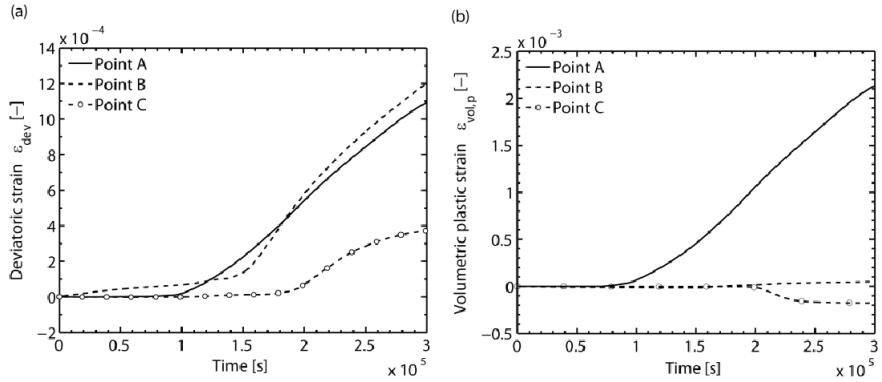

Figure 6. Evolution of deviatoric (a) and plastic volumetric (b) deformations.

Compared to the other observation points, the volumetric behaviour in point A is clearly distinguished. Point B situated in the middle part of the slope undergoes strong shearing of the same order of magnitude as for point A. The compressive plastic volumetric deformation at point B is however negligible. Point C located in the shearing zone running up to the slope surface reacts only after $2*10^5$ seconds. In accordance with the other observation points this suggests that the shearing mechanism starts in the lower part of the slope, above the abutment, then moves upwards along the bedrock interface and finally runs up to the slope surface, delimiting consequently a potentially unstable soil mass. The plastic volumetric strains in point C are negative in the sense of extension and are associated to the occurrence of plastic deviatoric strains. The extension of the soil can be either due to dilatancy during shearing, considering that the soil is overconsolidated, or due to a downwards movement of the potentially unstable soil mass leading to the formation of a tension crack in the upper part of the slope.

The almost normally consolidated soil in the lower part of the slope is a priori susceptible to plastic deformations in the sense of a wetting pore collapse. The wetting pore collapse is the property of the soils to get denser when soaked under a sufficient mechanical load. As shown in Figure 7a for points A and B the stress paths during wetting remain at first within

their respective elastic domains. The isotropic yield limits are reached at lower values of matric suction. The stress paths then follow the current isotropic yield surfaces without moving them noticeably. Yet, this process corresponds to soil hardening and generation of compressive volumetric plastic strains. This behaviour was experimentally observed in confined testing conditions and is coherent with the simulated conditions in the soil slope. There is a considerable loss in mean effective stress associated to the wetting pore collapse in point A after $7*10^4$ seconds which indicates a strength decrease in the lower part of the slope (Figure 7b). The mean effective stress reaches a constant value of around 60kPa after $1.5*10^5$ seconds. Matric suction decreases to a steady constant value of around 5kPa.

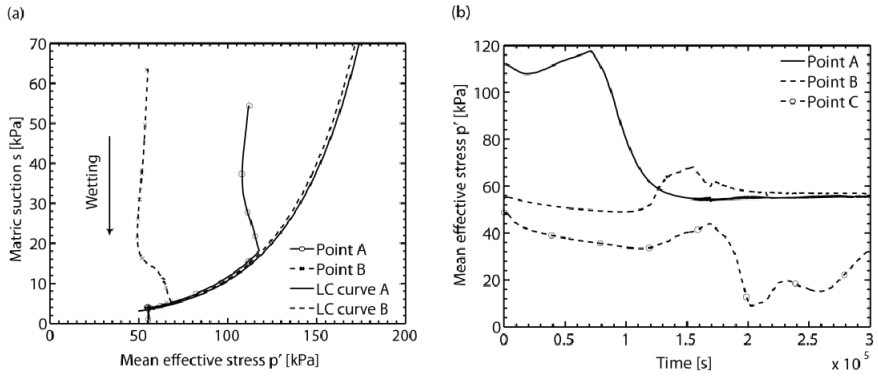

Figure 7. Stress paths and loading collapse curves (isotropic yield loci) for two points (a); Evolution of mean effective stresses (b).

To summarize, the deviatoric plastic mechanism is clearly predominant in the upper and middle part of the slope while in the lower part of the slope the isotropic plastic mechanism governs the behaviour.

5 CONCLUSIONS

Rainfall-induced shallow landslides often take place in slopes which are most of the time in a state of partial saturation. Although these failures take place rapidly, precursor signs in terms of surface settlements exist and have been observed in laboratory and field experiments (Take et al. 2004; Jia et al. 2009; Springman et al. 2009). In order to model numerically the onset of rainfall-induced landslides in variably saturated-unsaturated conditions, a consistent stress framework needs to be chosen. For this purpose, the generalized effective stress framework has been used. It allows on one hand a smooth transition between saturated and unsaturated states, and on the other an explicit hydromechanical coupling between the soil's effective stress and the evolution of matric suction and degree of saturation. The ACMEG-s model is capable of reproducing some of the major features of unsaturated soil behaviour, such as wetting pore collapse, soil shear strength and stiffness variation with matric suction. Its use for the transient finite element analysis of a partially saturated slope subjected to rain infiltration revealed interesting results on the actual onset of failure. The analysis gave detailed information on the active physical mechanisms during rain infiltration. The most probable failure mechanism develops in the lower part of the slope as a consequence of a wetting pore collapse and then spreads upwards along the bedrock and through the soil cover to the slope surface as a predominant shear mechanism. The volumetric compaction in the lower part of the slope is accompanied by important shear strains which indicate that both, isotropic and deviatoric plastic mechanisms are active. The increasing degree of saturation and the simultaneous volumetric compaction can also be interpreted as indicators for an increased susceptibility for flow mobilization in the post-failure stage.

ACKNOWLEDGEMENT

This work was supported by Swiss Competence Center Environment and Sustainability, TRAMM project and the European Commission, FP7 project SafeLand. Special thanks are addressed to Dr. F. Collin and Prof. R. Charlier from Université de Liège for their support in numerical issues.

REFERENCES

Askarinejad, A. (2009), "A method to locate the slip surface and measuring subsurface deformations in slopes". Proc. 4th Intern. Young Geotechnical Engineers' Conf., Alexandria.

Charlier, R. (1987), "Approche unifiée de quelques problèmes non linéaires de mécanique des milieux continus par la méthode des éléments finis". PhD thesis, Université de Liège.

Collin, F. (2003), "Couplages thermo-hydro-mécaniques dans les sols et les roches tendres partiellement saturés". PhD thesis, Université de Liège.

Dai Fuchu, Lee, C.F., and Wang Sijing (1999), "Analysis of rainstorm-induced slide-debris flows on natural terrain of Lantau Island, Hong Kong". Engineering Geology. 51 (4), 279–290.

Eichenberger, J., Nuth, M., Laloui, L. (2010), "Modeling landslides in partially saturated slopes subjected to rainfall infiltration". Chapter of the book "Mechanics of unsaturated geomaterials", pp.235-250, Eds. L. Laloui, John Wiley & Sons.

Godt J.W., Baum R.L., Lu N. (2009), "Landsliding in partially saturated materials". Geophysical Research Letters. 36, L02403, 1-5.

Hujeux, J. (1985), "Une loi de comportement pour le chargement cyclique des sols". Génie Parasismique. Paris, Les éditions de l'E.N.P.C.: 287-353.

Iverson, R.M., Reid, M.E., LaHusen, R.G. (1997), "Debris-flow mobilization from landslides". Annual Review of Earth and Planetary Sciences. 25, 85-138.

Jia, G.W., Zhan, T.L.T., Chen, Y.M., Fredlund, D.G. (2009), "Performance of a large-scale slope model subjected to rising and lowering water levels". Engineering Geology. 106, 92-103.

Johnson, K.A., Sitar, N. (1990), "Hydrologic conditions leading to debris flow initiation". Canadian Geotechnical Journal. 27 (6): 789-801.

Klubertanz, G., Laloui, L., Vulliet L. (2009), "Identification of mechanisms for landslide type initiation of debris flows". Engineering Geology. 109 (1-2), 114-123.

Laloui, L., Nuth, M. (2009), "On the use of the generalised effective stress in the constitutive modelling of unsaturated soils". Computer and Geotechnics. 36 (1-2): 20-23.

Nuth, M., Laloui, L. (2007), "New insight into the unified hydro-mechanical constitutive modelling of unsaturated soils". Proc. Unsat Asia 2007. Nanjing, 109-125.

Nuth, M., Laloui, L. (2008a), "Effective stress concept in unsaturated soils: Clarification and validation of a unified framework". International journal for numerical and analytical methods in Geomechanics. 32, 771-801.

Nuth, M., Laloui, L. (2008b), "Advances in modelling hysteretic water retention curve in deformable soils". Computers and Geotechnics. 35 (6), 835-844.

Schofield, A.N., Wroth, C.P. (1968), Critical state soil mechanics, McGraw-Hill, London.

Springman, S.M., Kienzler, P., Casini, F., Askarinejad, A. (2009), "Landslide triggering experiment in a steep forested slope in Switzerland". 17th Intern. Conf. of Soil Mech. & Geot. Eng., Alexandria.

Take, W.A., Bolton, M.D., Wong, P.C.P., Yeung, F.J. (2004), "Evaluation of landslide triggering mechanisms in model fill slopes". Landslides. 1 (3), 173-184.